Electronic Supplementary Information for

Regulation of Electrochemical Behaviors of Hierarchical Structured $Co_3(PO_4)_2$/Ni-Co-O for High-performance All-solid-state Supercapacitor

Tianxiang Yan,[a] Hanfang Feng,[a] Xueying Ma,[a] Lifeng Han, [a,c] Li Zhang*[a,b] and Shaokui Cao*[a,b]

[a]School of Materials Science and Engineering, Zhengzhou University, Zhengzhou 450001, People's Republic of China

[b]Henan Key Laboratory of Advanced Nylon Materials and Application, Zhengzhou University, Zhengzhou 450001, People's Republic of China.

[c]College of Materials and Chemical Engineering, Zhengzhou University of Light Industry, Zhengzhou 450002, People's Republic of China.

Experimental Section

Materials

Graphite powder (325 meshes) was bought from Qingdao Huatai Lubricant sealing S&T Co. Ltd. (Qingdao, China). Ferrite chloride hexahydrate ($FeCl_3$, 99.9%, metals basis), sodium hypophosphite (NaH2PO2·H2O, 99.9%, metals basis), dipotassium hydrogen phosphate (K_2HPO_4, 99.9%, metals basis), cobalt chloride hexahydrate ($CoCl_2 \cdot 6H_2O$, 99.9%, metals basis) were obtained from Beijing Chemical Reagent Factory (Beijing, China). Ni foam (NF, purity: 98%, thickness: 0.5 mm, mass density: 26 mg cm^{-2}) was purchased from Suzhou Taili Metal Foam Factory (Suzhou, China). All other reagents are of analytic grade, used as received without purification, and purchased from Shanghai Macklin Biochemical Co., Ltd.

Synthesis of $Co_3(PO_4)_2$/Ni-Co-O@NF (CPNO-12) hierarchical structure

$CoCl_2 \cdot 6H_2O$ (0.285 g, 1.2 mmol), K_2HPO_4 (0.137 g, 0.6 mmol) were dissolved in 10 mL distilled water and stirred vigorously for 0.5 hour to form a pink solution, afterwise the solution was transferred into a 20 mL Teflon-lined stainless autoclave with pure NF as supporter and collector, which was sealed and maintained at 150 °C for 12 hours and then allowed to cool to room temperature. In order to remove the surface NiO layer, NF (approximately 3 cm × 1 cm) was carefully cleaned with concentrated HCl solution (10 wt.%), acetone, absolute ethanol, deionized water (DI) in an ultrasound bath for 0.5 hour, respectively. CPNO with various reaction time were also prepared and noted as CPNO-x (x=3, 9, 12 and 15) depending on reaction hours. CPN-x (x=1, 1.5) were obtained under same condition as CPNO-12, except the ratio of cobalt to phosphate source: 1 and 1.5, respectively. All samples as-prepared were rinsed several times with distilled water and ethanol with the assistance of ultrasonication, and dried at 80 °C for 6 hours.

Synthesis of Fe_2P/graphene hydrogel@NF (FPGH)

Graphene Oxide (GO) was prepared by the oxidation of natural graphite powder using a modified Hummers method. The 5 mL graphene solution (2 mg mL^{-1}) and cleaned NF were transferred into a 20 mL autoclave and maintained at 180 °C for 12 hours to form a graphene hydrogel on NF. Then $FeCl_3$ (0.163 g, 1 mmol) and urea (1.2 g, 20 mmol) were dissolved in 20 mL distilled water and stirred to form a brown solution. Then as-prepared samples and the brown solution were transferred into a 20 mL Teflon-lined stainless-steel autoclave, which was sealed and maintained at 100 °C for 6 hours. Materials collected were rinsed several times with distilled water and ethanol with the assistance of ultrasonication, and dried at room temperature. Finally, the sample mixed with $NaH_2PO_2 \cdot H_2O$ (0.5 g, 5 mmol) were put into a quartz tube and annealed at 573 K for 2 hours at Ar atmosphere with a heating rate of 2 °C min^{-1}.

Measurements

X-ray powder diffraction (XRD) patterns were recorded on an X-ray diffractometer (D8 Advance (Bruker)) at a scan rate of 10° min^{-1} in the 2θ range from 10° to 80°. The morphology and X-ray energy dispersive spectrometer (EDS) analysis of the samples were characterized using a Hitachi S-8000 field-emission scanning electron

microscopy (FE-SEM) equipped with an X-ray energy dispersive spectrometer operating at 20 kV. To disclose the element distribution in CPNO-12, samples were scratched from the NF with knife and grinded for 0.5 hour with the assistance of ultrasonic bath to destroy the outer layer of samples before EDS analysis. High-resolution transmission electron microscopy (HRTEM) measurements were carried out using a JEOL model JEM 2010 EX microscopy at 200 kV. X-ray photoelectron spectroscopy (XPS) was carried out using an ESCALAB 250 photoelectron spectrometer (Thermo Fisher Scientific) with Al Ka (1486.6 eV) as the X-ray source set at 150 W and a pass energy of 30 eV for high resolution scan. BET surface area measurements were carried out using a Quantachrome Quadrasorb SI analyser. Raman spectra were collected from using a Raman Station (B&WTEK, BWS435-532SY) with a laser operating at 532 nm.

Three-electrode electrochemical tests

The electrochemical measurements were carried out at 298 K in a three-electrode glass cell connected to an electrochemical workstation. The active materials prepared in-situ on the NF (1 cm × 1 cm × 0.5 mm) were directly used as the working electrodes. A platinum electrode and an Hg/HgO electrode were used as counter and reference electrodes, respectively. Freshly prepared 1 M KOH aqueous solution was used as the electrolyte. CV curves (0~0.5 V, -1.2 V~0 for CPNO-12 and FPGH) and EIS (from 100 kHz to 10 mHz at open circuit voltage) spectra were recorded using an electrochemical workstation (CHI 660E). The GCD experiments were studied in a potential range of 0~0.5 V and -1.2 V~0 (*vs* Hg/HgO) for positive electrodes and negative electrodes, respectively.

All-solid-state asymmetric supercapacitors

All-solid-state asymmetric supercapacitors were fabricated using PVA-KOH gel as electrolyte and CPNO-12, FPGH as electrodes. Since the active materials were constructed in-situ on collectors and gel electrolyte serves as separators as well, extra polymer separators and conductive additive are avoided. The PVA-KOH gel electrolyte was prepared as following: 3.0 g PVA was added into 30 mL deionized water and heated to 90 °C for 60 minutes, then 5 mL KOH (4.5 g) solution was added slowly into the solution under stirring. The positive and negative electrodes were coated with the PVA-KOH gel solution and put into the vacuum oven for 1 hour to ensure full penetration of the as-obtained gel electrolyte. After the excess water was vaporized, the electrodes with solid-state electrolyte were sandwiched and covered with PTFE tape. Then, the flexible all-solid-state supercapacitors was successfully fabricated. Before carrying out electrochemical investigations, the electrodes were immersed in the prepared gel electrolyte for 1 hour. The energy density (E) and power density (P) of as-fabricated devices were calculated according to Equations S1 and Equation S2.

$$E = 1/2CV^2 \quad \text{(S1)}$$

$$P = E/t \quad \text{(S2)}$$

where C, V and t refer to capacity, potential window and discharge time, respectively.

Theoretical Calculations on Charge Storage Mechanism of CPNO-12

To understand the charge storage mechanism and determine which electrochemical behavior the CPNO-12 belongs to, theorectical calculations were conducted based on CV curves (as shown in Fig. S7 and Fig. 5c) according to following equations:

$$i_p = av^b \quad \text{(S3)}$$

$$\log i = b \log v \quad \text{(S4)}$$

where the peak current (i_p) obeys the power law relationships with scan rates (v), a and b refer to adjustable parameters. It's agreed that if b is equal to 0.5, the eletrochemical behavior is dominated by diffusion limited transfer process, termed as diffusion-controlled behavior (DCB); while if b=1, surface capacitive behavior (SCB) contribute most to the capacitance. [1-3] For analytic purposes, the Equation S3 is simplified to Equation S4 to determine the value of b; as plotted in Fig. 4g, value of b is calculated to be 0.71, indicating the coexistance of DCB and SCB in CPNO-12.

Exact contributions from DCB and SCB has also been calculated based on Equation S5, which can be transformed into a simplified form, Equation S6.

$$i(V) = k_1 v + k_2 v^{\frac{1}{2}} \quad \text{(S5)}$$

$$\frac{i(V)}{v^{\frac{1}{2}}} = k_1 v^{\frac{1}{2}} + k_2 \quad \text{(S6)}$$

The value of $k_1 v$ and $k_2 v^{1/2}$ represent contributions from CB and DCB, respectively. According to Equation S6, by plotting the v versus i at specific potentials, corresponding value of k_1 and k_2 can be determined by slopes and y-axis intercept of straight lines.[4-7] Then capacity contributions from SCB in CPNO-12 and CPNO-3 are determined according to the procedure discussed above, the results of which are given in Fig. 4i and Fig. S8.

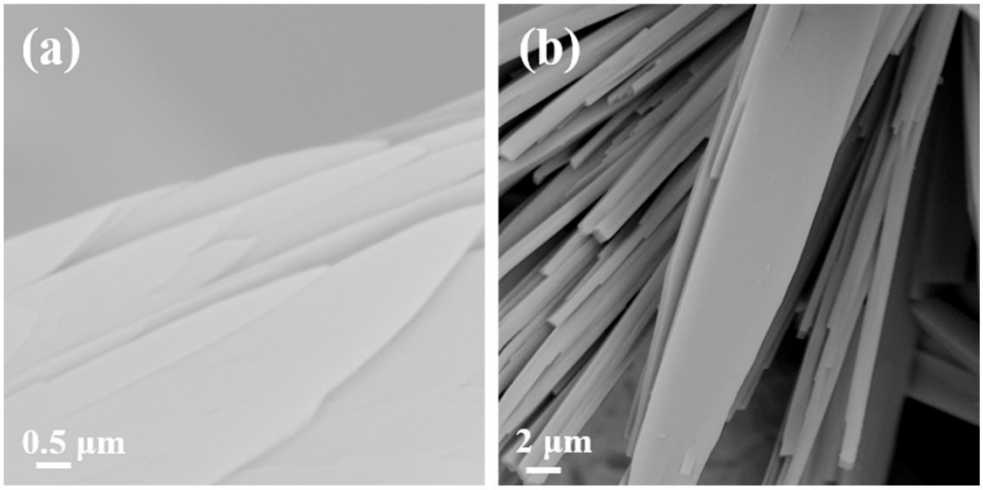

Fig. S1 SEM images of (a) CPN-1 and (b) CPN-1.5.

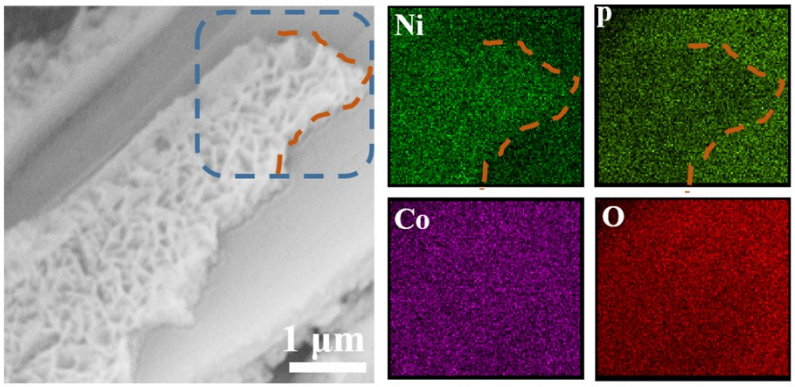

Fig. S2 SEM images and corresponding EDS analysis of CPNO-12.

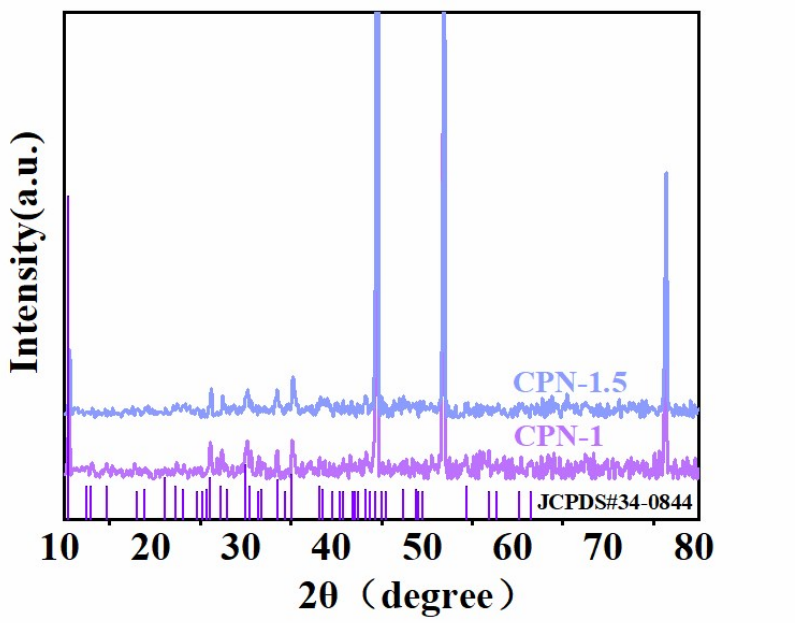

Fig. S3 XRD pattern of CPN-x (x=1, 1.5) and corresponding standard data of $Co_3(PO_4)_2{\cdot}4H_2O$ (JCDPS No. 34-0844).

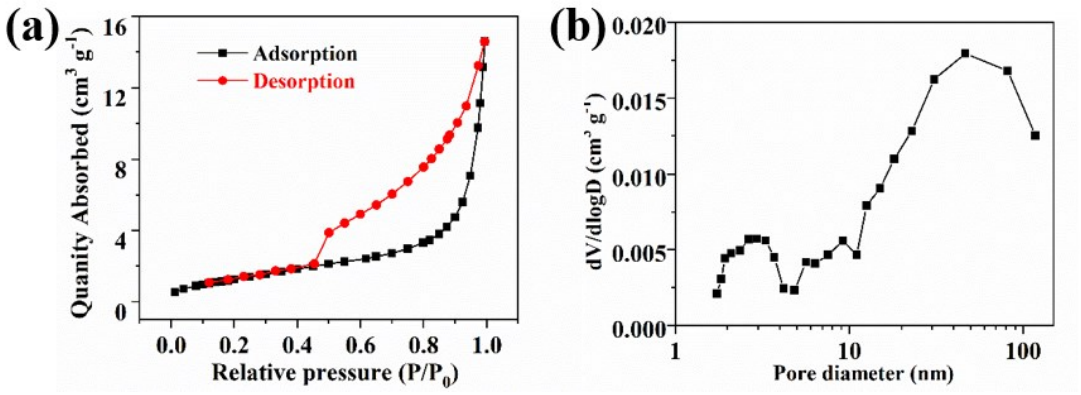

Fig. S4 (a) The N_2 sorption-desorption isothermal analysis and (b) pore size distribution of CPNO-12.

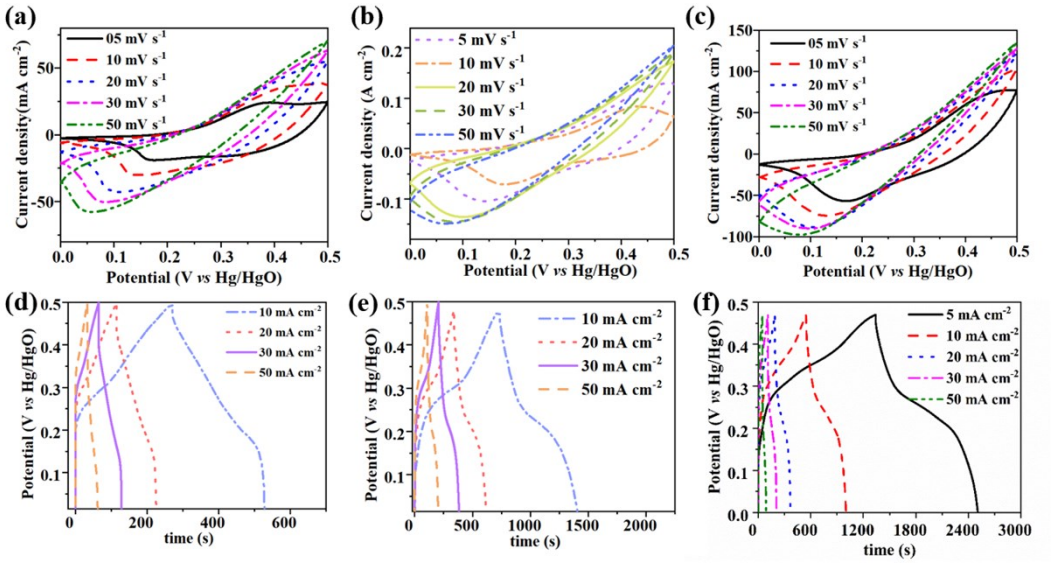

Fig. S5 CV curves of (a) CPNO-3, (b) CPNO-9, (c) CPNO-15 at various scan rates; GCD curves of (d) CPNO-3, (e) CPNO-9, (f) CPNO-15 at various current density.

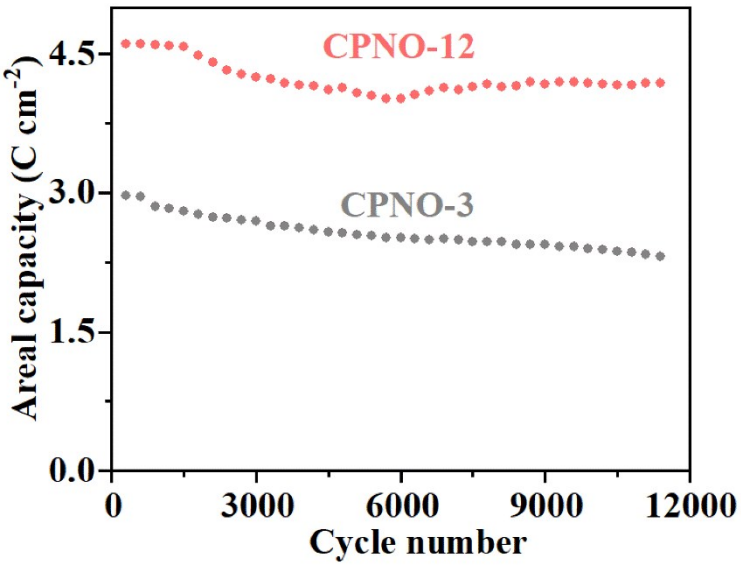

Fig. S6 Cyclability of CPNO-12 and CPNO-3 at 50 mA cm^{-2} after 12000 cycles.

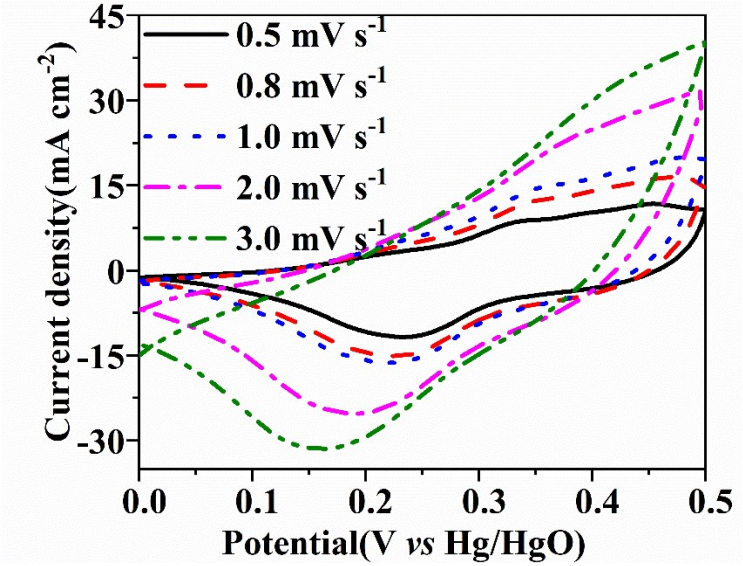

Fig. S7 CV curves of CPNO-12 at low scan rates (0.5~3 mV s^{-1}).

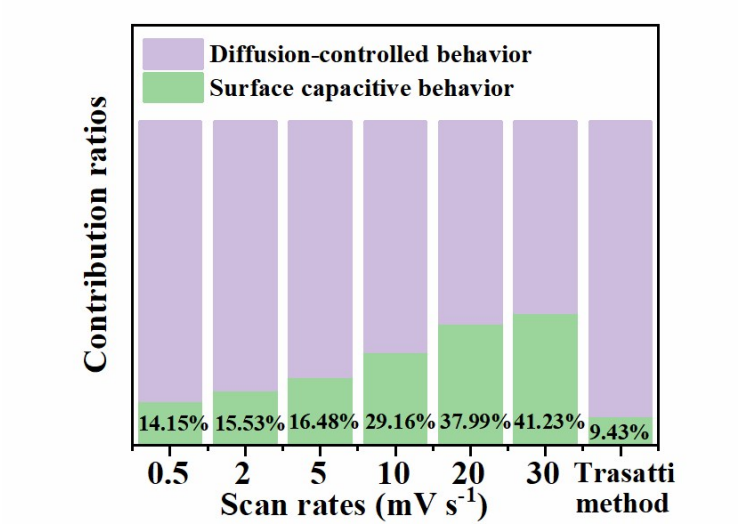

Fig. S8 Capacity contributions from DCB and SCB in CPNO-3.

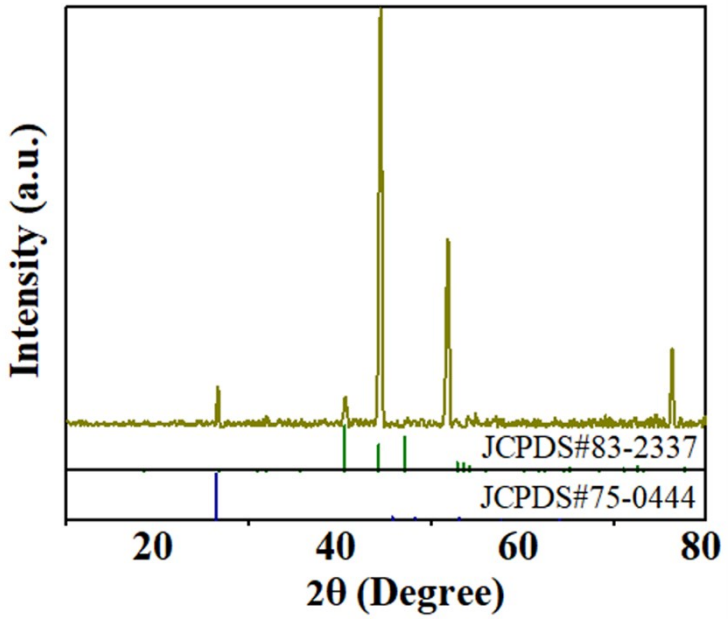

Fig. S9 XRD pattern of FPGH, and the corresponding standard pattern of Fe_2P (JCPDS No. 83-2337) and graphite carbon (JCPDS No.75-0444).

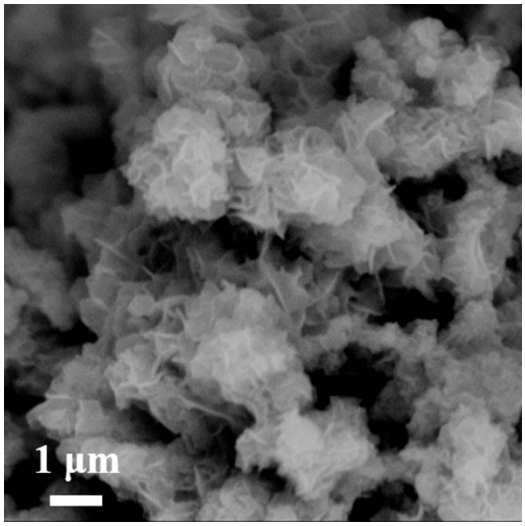

Fig. S10 SEM image of FPGH.

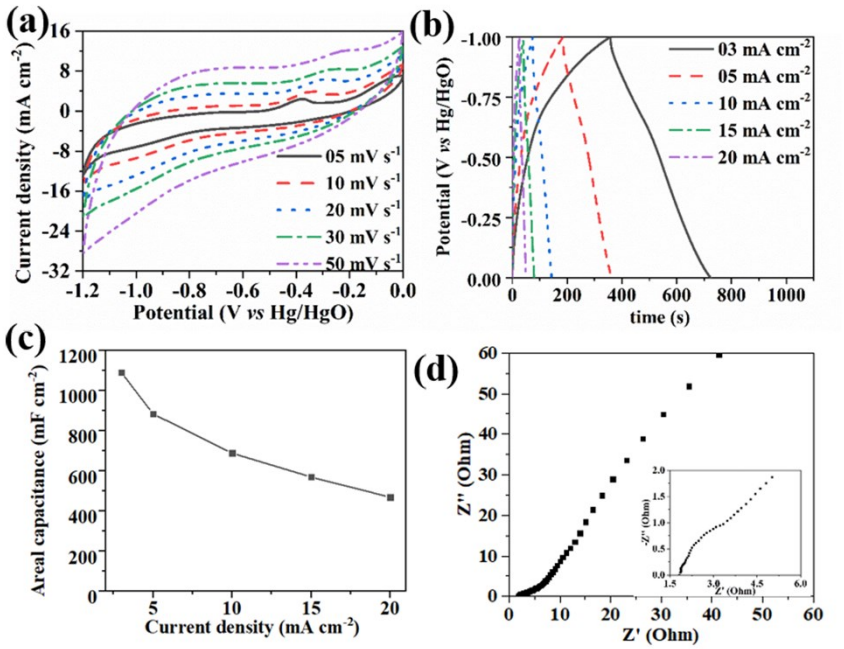

Fig. S11 Electrochemical performance of FPGH. (a) CV curves and (b) GCD curves of FPGH at various scan rates and current densities, respectively; (c) rate capacity of FPGH; (d) EIS curves of FPGH (inset: EIS curve at high frequency region).

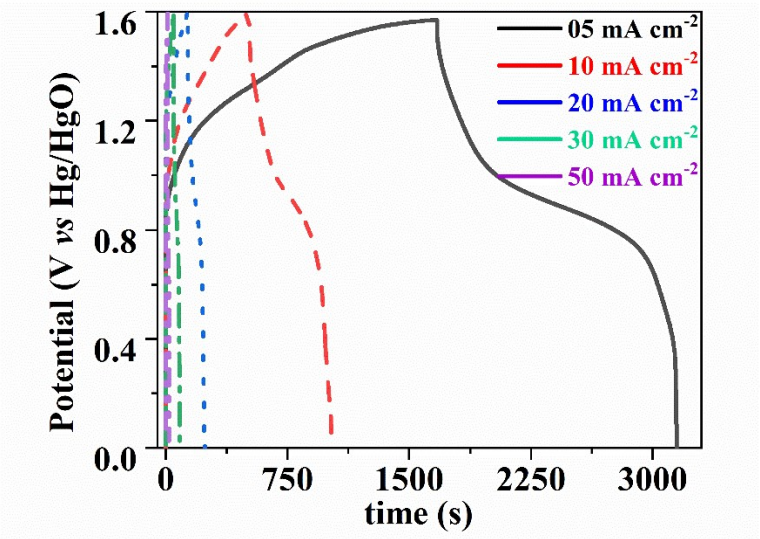

Fig. S12 GCD curves of CPNO//FPGH ASSSC device at various current density (5~50 mA cm^{-2}).

Fig. S13 The LED powered by solo CPNO//FPGH ASSSC device.

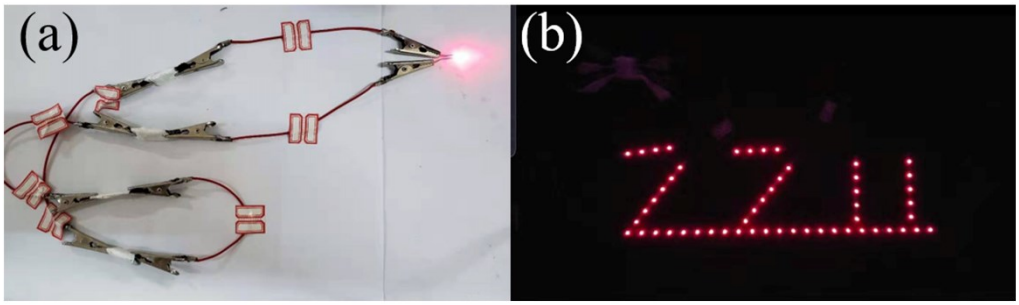

Fig. S14 (a) the single LED and (b) LED lighting set powered by tandem CPNO//FPGH ASSSC devices.

Notes and references

1. H. Yin, C. Song, Y. Wang, S. Li, M. Zeng, Z. Zhang, Z. Zhu and K. Yu, *Electrochim. Acta* **2013**. *111*, 762.
2. J. Duay, S. A. Sherrill, E. Gillette and S. B. Lee, *ACS Nano* **2013**. *7*, 1200.
3. X. Yin, C. Zhi, W. Sun, L. P. Lv and Y. Wang, *J. Mater. Chem. A* **2019**. *7*, 7800.
4. G. Zou, H. Hou, J. Hu and X. Ji, *Batteries Supercaps*, **2019**. *2*, 712.
5. T. Brezesinski, J. Wang, J. Polleux, B. Dunn and S. H. Tolbert, *J. Am. Chem. Soc.* **2009**. *131*, 1802.
6. H. S. Kim, J. B. Cook, H. Lin, J. S. Ko, S. H. Tolbert, V. Ozolins and B. Dunn, *Nat. Mater.* **2017**. *16*, 454.
7. K. A. Owusu, L. Qu, J. Li, Z. Wang, K. Zhao, C. Yang, K. M. Hercule, C. Lin, C. Shi, Q. Wei, L. Zhou and L. Mai, *Nat. Commun*. **2017**. *8*, 14264.